

# Elastic Anisotropic and Thermodynamic Properties of $I-4m2$ -BCN

MENGJIANG XING\*, BINHUA LI, ZHENGTTAO YU AND QI CHEN

Faculty of Information Engineering and Automation, Kunming University of Science and Technology,  
Kunming, 650051, China

(Received October 26, 2014; in final form March 20, 2016)

Based on the density functional theory and the quasi-harmonic Debye model, the structural and thermodynamic properties of  $I-4m2$ -BCN have been studied in this paper. Some structural parameters are presented in this work. All of these results are in excellent agreement with the other available results. The anisotropy of elastic properties are also studied systematically in this paper. Finally, the thermodynamic properties of  $I-4m2$ -BCN are also researched through the quasi-harmonic Debye model. The relations among the thermal expansion  $\alpha$ , the Debye temperature  $\Theta_D$ , the heat capacity  $C_V$  and  $C_P$ , the Grüneisen parameter  $\gamma$ , entropy  $S$ , and the Gibbs free energy  $G$  with pressure  $P$  and temperature  $T$  are studied systematically.

DOI: [10.12693/APhysPolA.129.1124](https://doi.org/10.12693/APhysPolA.129.1124)

PACS/topics: 62.20.de, 63.20.dk, 65.40.-b, 71.15.Mb

## 1. Introduction

New covalent boron–carbon–nitrogen (BCN) materials and related nanostructures occupy a privileged position amongst candidates for high-temperature optical, electrical, and mechanical applications [1]. In particular, ternary boron carbonitride ( $BC_xN_y$ ) solid solutions have attracted considerable interest in the last decades as alternatives to increase the performance of elemental (diamond, graphite,  $\alpha$ -rh boron, etc.) and binary (c-BN,  $B_4C$ , h-BN, h-CN<sub>x</sub>, etc.) phases of the BCN system. Due to its high technological potential,  $BC_xN_y$  thin films have been created by several chemical [2–13] deposition methods. Recent experiments announced successful synthesis of cubic boron–carbonitride compounds  $BC_2N$  with an ultra hardness second only to diamond. In that present letter, of Zhang et al. [14], their results reveal that, despite the large elastic constants, compositional anisotropy and strain dependent bonding character impose limitation on their strength. Consequently, the hardness of this  $BC_2N$  phase is lower than that of c-BN, the second hardest material as we all know. When the BCN films were deposited by using ion beam assisted evaporation, Zhou et al. [15] have reported the lower evaporation rate of  $B_4C$  target, the smaller surface roughness and higher nanohardness of BCN coatings. But if the BCN films were deposited by using dual ion beam sputtering (DIBS), their hardness was mainly affected by carbon sputtering power, working pressure and boron sputtering power in sequence [16].

The structural, elastic, and elastic anisotropy properties of  $R3-B_2C$  [17] and  $I4mm-B_3C$  [18] were investigated using first-principles density functional calculations by

Fan et al. The Vickers hardness of  $R3-B_2C$  and  $I4mm-B_3C$  is 51 GPa and 42 GPa [19], respectively. Therefore,  $R3-B_2C$  and  $I4mm-B_3C$  are potential superhard materials.

The thermodynamic properties of  $R3-B_2C$  and  $I4mm-B_3C$  were investigated utilizing the quasi-harmonic Debye model. Chang et al. [20] have studied the thermodynamic properties of the potential superhard  $\beta$ - $BC_2N$  in orthorhombic structure by using *ab initio* plane-wave pseudopotential density functional theory method. They investigate through the quasi-harmonic Debye model the thermodynamic properties of  $\beta$ - $BC_2N$ . All of these results are in excellent agreement with the available experimental and other theoretical results. Recently, the mechanical and electronic properties of  $P3m1$ -BCN [21] have been studied by using first principles calculations. The anisotropy studies of Young's modulus, shear modulus and Poisson's ratio show that  $P3m1$ -BCN exhibits a large anisotropy. Electronic structure study shows that  $P3m1$ -BCN is an indirect semiconductor with band gap of 4.10 eV. In addition,  $P3m1$ -BCN still keeps brittle in this pressure range from 0 to 100 GPa.

Zhang et al. [22] reported a developed methodology to design superhard materials for given chemical systems under external conditions. Based on density function theory in the frame of the local density approximation and the generalized gradient approximation, Fan et al. [23] have systematically studied the structural stability, elastic properties, and mechanical properties of BCN compounds with  $I4mm2$  and  $I-4m2$  phases. They found that  $I-4m2$ -BCN is mechanically and dynamically stable. In this work, the researchers will focus on studying the thermodynamic properties and elastic anisotropic properties of BCN in  $I-4m2$  phase (space group:  $I-4m2$ , No. 119) based on quasi-harmonic Debye model and the elastic anisotropy measures (ELAM).

\*corresponding author; e-mail: [mjxing168668@163.com](mailto:mjxing168668@163.com)

## 2. Theoretical method

### 2.1. Total energy electronic structure calculations

In our calculations, the structural optimization and property predictions of the BCN polymorphs were performed using the DFT [24, 25] with the generalized gradient approximation (GGA) parametrized by Perdew, Burke and Ernzerhof (PBE) [26] as implemented in the Cambridge Serial Total Energy Package (CASTEP) code [27]. For *I-4m2*-BCN, we used a plane-wave basis set with energy cut-off 500 eV, used with GGA. For the Brillouin-zone sampling, the  $6 \times 6 \times 4$  Monkhorst–Pack mesh [28] is adopted. The Broyden–Fletcher–Goldfarb–Shanno (BFGS) [29] minimization scheme was used in geometry optimization. The self-consistent convergence of the total energy is  $5 \times 10^{-6}$  eV/atom, the maximum force on the atom is 0.01 eV/Å, the maximum ionic displacement within  $5 \times 10^{-4}$  Å and the maximum stress within 0.02 GPa. From these calculations, the energy zero for a unit formula is obtained, in Ha per molecule and volume per unit formula, in Bohr<sup>3</sup> per molecule.

### 2.2. The quasi-harmonic Debye model

For the thermodynamic properties of *I-4m2*-BCN, the quasi-harmonic Debye model [30–33] is applied. In the quasi-harmonic Debye model, the non-equilibrium Gibbs function  $G^*(V : P, T)$  is given by

$$G^*(V : P, T) = E(V) + PV + A_{\text{vib}}(\Theta_D(V) : T). \quad (1)$$

Here  $E(V)$  represents the total energy per unit cell for *I-4m2*-BCN,  $\Theta_D$  represents the Debye temperature, and the vibrational Helmholtz free energy  $A_{\text{vib}}$  can be written by [34–39]:

$$A_{\text{vib}}(\Theta_D(V) : T) =$$

$$nKT \left[ \frac{9}{8} \frac{\Theta_D}{T} + 3 \ln(1 - e^{-\Theta_D/T}) - D \left( \frac{\Theta_D}{T} \right) \right]. \quad (2)$$

Here  $D(\Theta_D/T)$  represents the Debye integral. Assume that  $y$  is equal to  $\Theta_D/T$ , so

$$D(y) = \frac{3}{y^3} \int_0^y \frac{x^3}{e^x - 1} dx, \quad (3)$$

$n$  represents the number of atoms per formula unit and  $\Theta_D$  is expressed as [34]:

$$\Theta_D = \frac{h}{2\pi k} [6\pi^2 V^{1/2} n]^{1/3} f(v) \sqrt{\frac{B_s}{M}}, \quad (4)$$

where  $M$  represents the molecular mass per formula unit,  $B_s$  represents the adiabatic bulk modulus, the Poisson ratio  $v$  is taken as 0.11 in our calculation, and  $f(v)$  is given

by [35, 36]:

$$f(v) = 3 \left[ 2 \left( \frac{2}{3} \frac{1+v}{1-2v} \right)^{3/2} + \left( \frac{1}{3} \frac{1+v}{1-v} \right)^{3/2} \right]^{-1}. \quad (5)$$

Therefore, the non-equilibrium Gibbs function  $G^*(V : P, T)$  as a function of  $(V : P, T)$  can be minimized with respect to volume  $V$  as follows:

$$\left( \frac{\partial G^*(V : P, T)}{\partial V} \right)_{P, T} = 0. \quad (6)$$

By solving Eq. (6), the isothermal bulk modulus and other thermal properties such as heat capacity at constant volume  $C_V$ , the heat capacity at constant pressure  $C_P$ , and thermal expansion  $\alpha$  are respectively taken as [40]:

$$B_T = -V \left( \frac{\partial P}{\partial V} \right) = V \left( \frac{\partial^2 G^*(V : P, T)}{\partial V^2} \right)_{P, T} = -x^{-2} B_0 e^{a(1-x)} f(x), \quad (7)$$

$$x = \left( \frac{V}{V_0} \right)^{1/3}, \quad (8)$$

$$f(x) = x - 2 - ax(1-x), \quad (9)$$

where  $V_0 = V(0, T)$  is the zero-pressure equilibrium volume,  $B_0$  is the zero-pressure bulk modulus, and  $a$  is given through the relation

$$a = 3(B'_0 - 1)/2, \quad (10)$$

where  $B'_0$  represents the first pressure derivative. In addition,  $B_0$ ,  $\ln B'_0$  and  $\alpha$  are the fitting parameters. Also

$$C_V = 3nk \left[ 4D \left( \frac{\Theta_D}{T} \right) - \frac{3\Theta_D/T}{e^{\Theta_D/T} - 1} \right], \quad (11)$$

$$C_p = C_V(1 + \alpha\gamma T), \quad (12)$$

$$\alpha = \frac{\gamma C_V}{B_T V}, \quad (13)$$

where  $C_V$  represents the heat capacity and  $\gamma$  represents the Grüneisen parameter and it is expressed as

$$\gamma = -(d \ln \Theta_D(V) / d \ln V). \quad (14)$$

## 3. Results and discussion

### 3.1. Structural properties and elastic properties

The calculated lattice parameters for *I-4m2*-BCN, are presented in Table I. *I-4m2*-BCN has a tetragonal symmetry that belongs to the *I-4m2* space group. For *I-4m2*-BCN, the calculated lattice parameters are in excellent agreement with the reported calculated results [22, 23].

TABLE I

Calculated equilibrium lattice parameters  $a$ ,  $c$ ,  $V$ , elastic constants  $C_{ij}$  (in GPa) for *I-4m2*-BCN.

Phase	Method	$a$	$c$	$V$	$C_{11}$	$C_{12}$	$C_{13}$	$C_{33}$	$C_{44}$	$C_{66}$	$B$	$G$
<i>I-4m2</i>	GGA <sup>a</sup>	2.56	10.99	18.07	858	49	135	756	379	330	344	359
	LDA <sup>a</sup>	2.53	10.84	17.34	936	52	155	806	424	346	376	386
	GGA <sup>b</sup>	2.57	11.00	18.12								

<sup>a</sup>this work, <sup>b</sup>Ref. [22].

The lattice parameters and elastic constants  $C_{ij}$ , bulk modulus  $B$ , and shear modulus  $G$  were calculated in present works, using the Voigt–Reuss–Hill approximation [41], with GGA for  $I-4m2$ -BCN are also presented in Table I. The criteria for mechanical stability of tetragonal phase are given by [42]:  $C_{ii} > 0$ ,  $i = 1, 3, 4, 6$ ;  $(C_{11} - C_{12}) > 0$ ;  $(C_{11} + C_{33} - 2C_{13}) > 0$ ;  $[2(C_{11} + C_{12}) + C_{33} + 4C_{13}] > 0$ . The calculated elastic constants of  $I-4m2$ -BCN indicated that it is mechanically stable due to the satisfaction of the mechanical stability criteria.

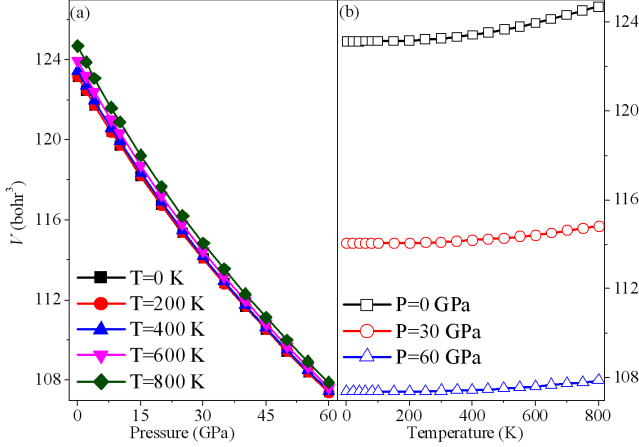


Fig. 1. Pressure (a) and temperature (b) dependence of the equilibrium volume for the  $I-4m2$ -BCN.

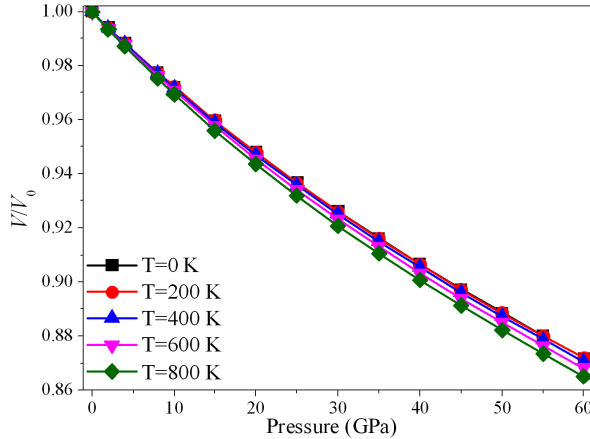


Fig. 2. The equilibrium volume  $V/V_0$  of  $I-4m2$ -BCN as a function of pressure at  $T = 0, 200, 400, 600,$  and  $800$  K.

Total energy calculations are done as a function of increasing and reducing unit cell volume around equilibrium cell volume ( $V_0$ ) and obtained data for  $E - V$  by fitting it into the Murnaghan equation of states (EOS) [43]. Figure 1a shows the relations of the volume as a function of pressure  $P$  up to 60 GPa at  $T = 0, 200, 400, 600,$  and  $800$  K, and the relationship between volume  $V$  and tem-

perature  $T$  at different pressures  $P = 0, 30,$  and  $60$  GPa are shown in Fig. 1b. In Fig. 1a, volume  $V$  decreases with pressure at certain temperature. One can obviously see that when  $T < 400$  K,  $V$  keeps nearly constant; when  $T > 400$  K,  $V$  increases as  $T$  increases. From Fig. 1 we can find that the effect of the temperature  $T$  on the volume  $V$  is less significant than that of pressure  $P$  on it. The primitive cell volumes  $V/V_0$  of  $I-4m2$ -BCN as a function of pressure  $P$  at  $T = 0, 200, 400, 600,$  and  $800$  K are shown in Fig. 2. Correspondingly, in Fig. 2, when  $T < 400$  K, the primitive cell volume  $V/V_0$  of  $I-4m2$ -BCN has a little change; when  $T > 400$  K, the cell volume  $V/V_0$  changes obviously as  $T$  increases. From Fig. 2, it is found that the effect of temperature on the ratio  $V/V_0$  is not as significant as that of pressure in our calculated pressure and temperature ranges.

### 3.2. Thermodynamic properties

The investigation on the thermodynamic properties of solids under high pressure and high temperature is an interesting topic in the condensed matter physics. The investigations on the thermodynamic properties of  $I-4m2$ -BCN under high temperature and pressure are determined by the quasi-harmonic Debye model. The thermodynamic properties of  $I-4m2$ -BCN are determined in the temperature range from 0 to 800 K where the quasi-harmonic model remains fully valid. Meanwhile, the pressure effect is studied in the range 0–60 GPa.

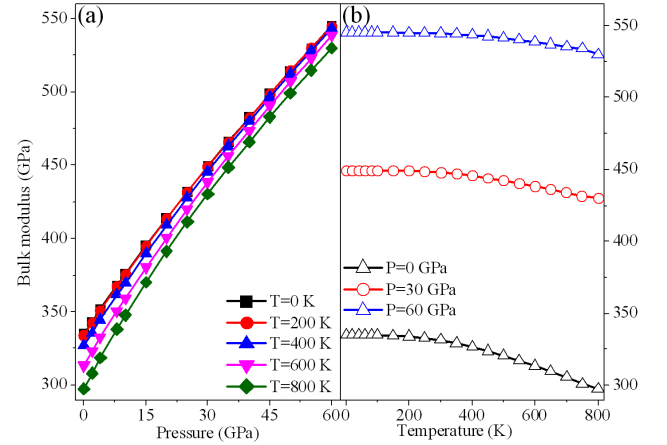


Fig. 3. Variation of the isothermal bulk modulus of  $I-4m2$ -BCN versus pressure and temperature.

Here we focus our attention on the dependence of isothermal bulk modulus  $B_T$  on pressure and temperature through the quasi-harmonic Debye model. Figure 3a shows the relations of the isothermal bulk modulus  $B_T$  as a function of pressure  $P$  up to 60 GPa at  $T = 0, 200, 400, 600,$  and  $800$  K, and the relationship between isothermal bulk modulus  $B_T$  and temperature  $T$  at different pressures  $P = 0, 30,$  and  $60$  GPa are shown in Fig. 3b. In Fig. 3a, isothermal bulk modulus  $B_T$  increases with pressure at certain temperature. In both

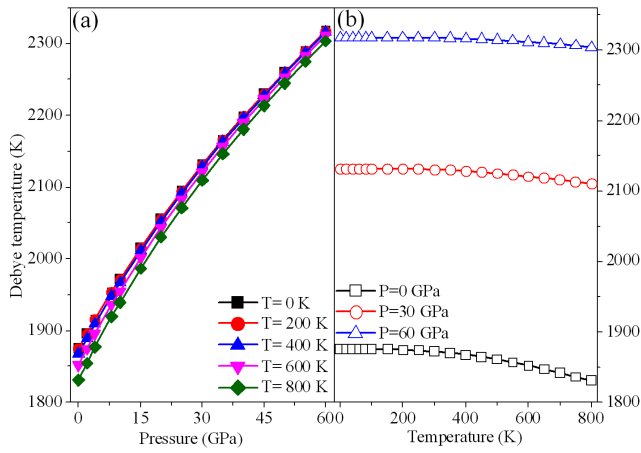


Fig. 4. Variation of the Debye temperature of  $I-4m2$ -BCN versus pressure and temperature.

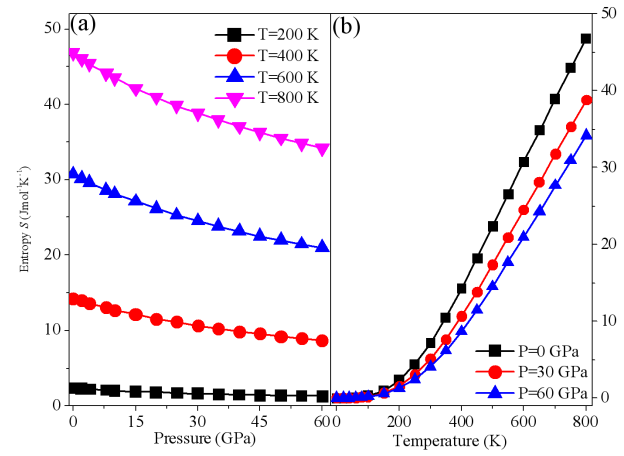


Fig. 7. Variation of the entropy of  $I-4m2$ -BCN versus pressure and temperature.

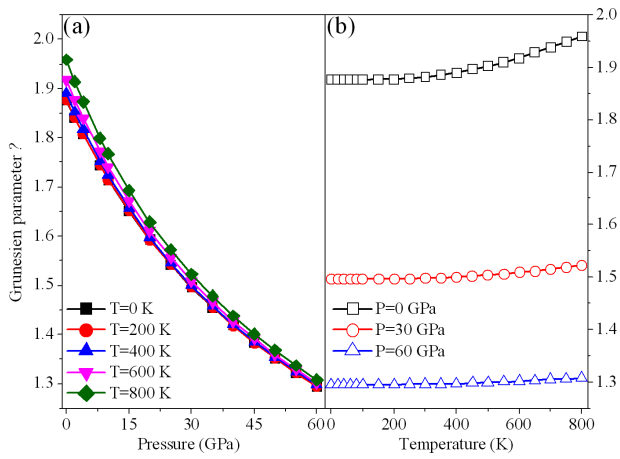


Fig. 5. Variation of the Grüneisen parameter  $\gamma$  of  $I-4m2$ -BCN versus pressure and temperature.

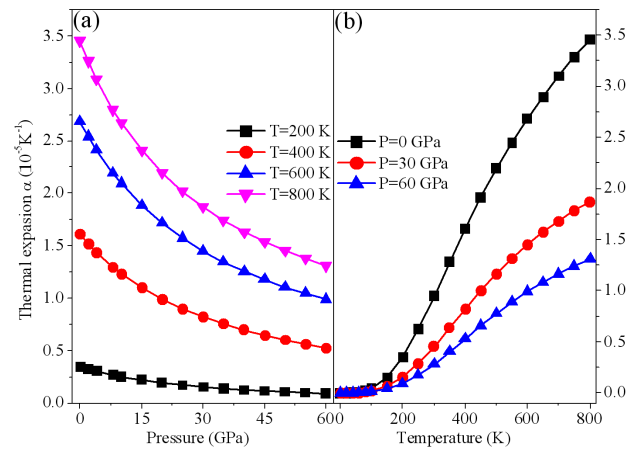


Fig. 8. Variation of the thermal expansion of  $I-4m2$ -BCN versus pressure and temperature.

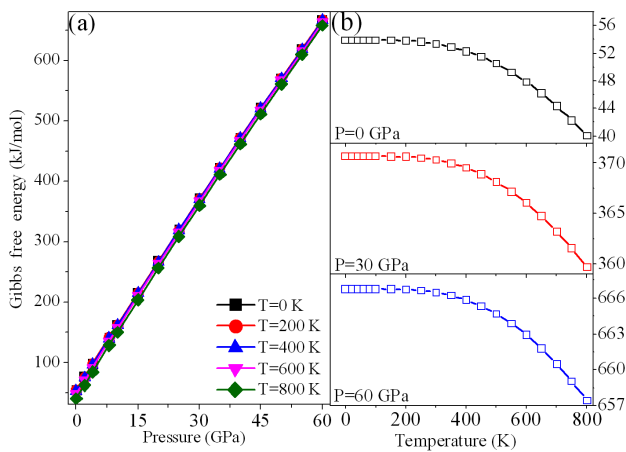


Fig. 6. Variation of the Gibbs free energy of  $I-4m2$ -BCN versus pressure and temperature.

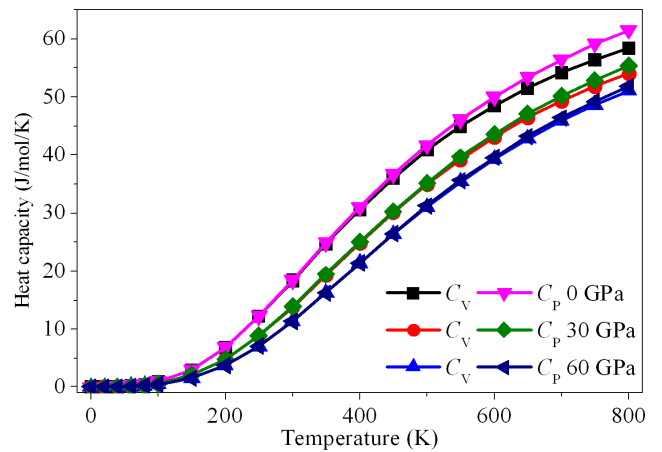


Fig. 9. Variation of the heat capacity of  $I-4m2$ -BCN versus pressure and temperature.

Fig. 3a and b, it can be seen that isothermal bulk modulus  $B_T$  remains almost unchanged with temperature at pressures  $P = 30$  GPa, and 60 GPa. It can be obviously seen that with  $T > 200$  K,  $B_T$  remains basically unchanged; with  $T > 200$  K,  $B_T$  decreases as  $T$  increases. As well as shown in Fig. 3, it can be find out that the effect of the temperature  $T$  on the isothermal bulk modulus is less significant than that of pressure  $P$  on it.

In the quasi-harmonic Debye model, the Debye temperature and the Grüneisen parameter are the two key quantities. The Debye temperature relates closely to many physical properties of solids, such as specific heat, dynamic properties, and melting temperature. The calculated relationships of the Debye temperature on pressure and temperature are plotted in Fig. 4. Shown in Fig. 4a, it can be seen that the Debye temperature increases monotonously at given temperature. It is clearly seen that the Debye temperature decreases with temperature at certain pressure shown in Fig. 4b. The lower the pressure is, the faster the Debye temperature decreases. Varying temperature from 0 to 800 K, the Debye temperature decreases 2.36% at 0 GPa and 0.60% at 60 GPa.

The Grüneisen parameter  $\gamma$ , which describes the alteration in a crystal lattices vibration frequency, can reasonably predict the anharmonic properties of a solid, such as the temperature dependence of phonon frequencies and lattice volume. Usually, the Grüneisen parameter is positive and lies in the range  $1.5 \pm 1.0$ . The calculated relationships of the Grüneisen parameter on pressure and temperature are plotted in Fig. 5. It is found that the Grüneisen parameter decreases with pressure at a given temperature, but increases with temperature at a given pressure. The Grüneisen parameter almost decreases linearly with pressure. At low temperature ( $T < 250$  K), the Grüneisen parameter is constant, as well as increases linearly with temperature at high temperature ( $T > 400$  K).

In thermodynamics, the Gibbs free energy [44] is a thermodynamic potential that measures the “usefulness” or process-initiating work obtainable from a thermodynamic system at a constant temperature and pressure. When a system varies from a well-defined original state to a well-defined final state, the Gibbs free energy equals the work exchanged by the system with its surroundings, minus the work of the pressure forces, during a reversible transformation of the system from the same initial state to the same final state [45]. Figure 6a shows the Gibbs free energy of  $I-4m2$ -BCN as a function of pressure at different temperatures, and Fig. 6b shows Gibbs free energy of  $I-4m2$ -BCN as a function of temperature at different pressures. It can be seen that at a given temperature, Gibbs free energy increases widely with the increment of the pressures. The Gibbs free energy becomes level with increasing temperature ( $T < 200$  K) and then decreases sharply ( $T > 200$  K).

In thermodynamics, entropy  $S$  is a measure of the number of specific ways in which a thermodynamic system may be arranged, often taken to be a measure of

disorder, or a measure of progressing towards thermodynamic equilibrium. The variation of the entropy  $S$  versus temperature and pressure for  $I-4m2$ -BCN is displayed in Fig. 7. It is shown that  $S$  decreases with the increase of pressure and increases sharply with an increasing temperature. As temperature increases, the entropy increases quickly at lower pressure. As pressure increases, the entropy decreases quickly at higher temperature and as temperature increases, the entropy increases quickly at lower pressure.

The coefficient of thermal expansion  $\alpha$  describes how the size of an object changes with a change in temperature. Specifically, it measures the fractional change in size per degree of change in temperature at a constant pressure. For solids, one might only be concerned with the change along a length, or over some area. The calculated relationships of thermal expansion coefficient  $\alpha$  on pressure and temperature are plotted in Fig. 8 for  $I-4m2$ -BCN. It can be noted that, at a given pressure,  $\alpha$  increases sharply with the increase of temperature up to 100 K. When  $T > 100$  K,  $\alpha$  gradually approaches a linear increase with enhanced temperature which means that the temperature dependence of  $\alpha$  is large at a high temperature. For a given temperature,  $\alpha$  decreases with the increase of pressure. At 300 K and zero pressure,  $\alpha$  is equal to  $0.95 \times 10^{-5} \text{ K}^{-1}$ . The effects of pressure on the thermal expansion coefficient are very small at low temperatures, and the effects increase with the increase of temperature.

The temperature dependence of the calculated heat capacity  $C_V$  and  $C_P$  at various pressures are shown in Fig. 9. Due to the anharmonic approximations of the Debye model, the heat capacity  $C_V$  and  $C_P$  increase rapidly with pressure. At low temperature ( $T < 400$  K), the difference between  $C_V$  and  $C_P$  is slight,  $C_V$  is proportional to  $T^3$ . It is also interesting to note that the values of  $C_V$  follow the Debye model at low temperature due to the anharmonic approximations. In a word, it can be seen that the heat capacity increases with the temperature at certain pressure and decreases with the pressure at certain temperature. The influences of the temperature on the heat capacity are much more significant than that of the pressure on it.

### 3.3. Anisotropic properties

Using the elastics anisotropy measures [46], we can obtain the calculated Poisson ratio, shear modulus and Young modulus along different directions as well as the projections in different planes. It is the Poisson ratio that was first focused on, and Fig. 10a–c displays the 2D representation of the Poisson ratio in the  $xy$ ,  $xz$ , and  $yz$  planes for  $I-4m2$ -BCN, respectively. The black represents maximum and red represents minimum. It was found that  $0.03 \leq v \leq 0.17$ , showing that  $v$  remains positive. In order to quantify the anisotropy, we calculated the shear modulus for all possible directions of shear strain, the 2D representation of shear modulus in the  $xy$ ,  $xz$ , and  $yz$  planes for  $I-4m2$ -BCN are shown in

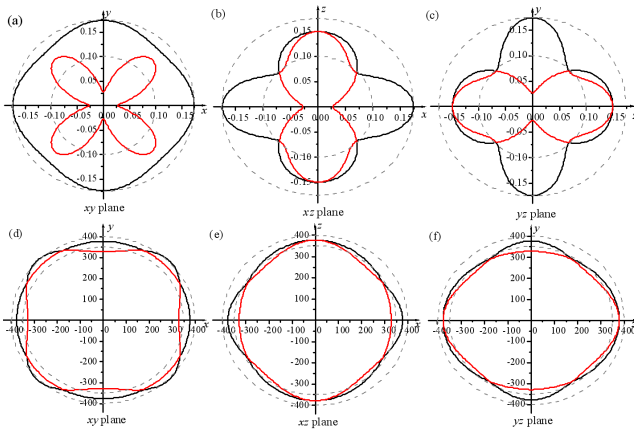


Fig. 10. 2D representation of the Poisson ratio in the  $xy$  plane (a),  $xz$  plane (b) and  $yz$  plane (c) for  $I-4m2$ -BCN. 2D representation of shear modulus in the  $xy$  plane (d),  $xz$  plane (e), and  $yz$  plane (f) for  $I-4m2$ -BCN.

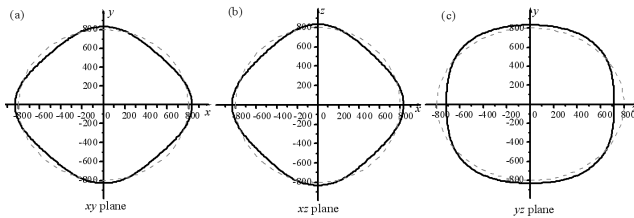


Fig. 11. 2D representation of the Young modulus in the  $xy$  plane (a),  $xz$  plane (b) and  $yz$  plane (c) for  $I-4m2$ -BCN.

Fig. 10d–f, respectively. The black represents maximum and red represents minimum. It was observed that shear modulus varies between 329 and 405 GPa, the average value of all directions is 356 GPa. Finally, it is focused on Young's modulus, which is shown the 2D representation of Young's modulus in the  $xy$ ,  $xz$ , and  $yz$  planes for  $I-4m2$ -BCN in Fig. 11a–c, respectively. It is clearly visible that Young's modulus for this material is large anisotropic, with a minimal value of  $E_{\min} = 715$  GPa and a maximum of  $E_{\max} = 846$  GPa. So  $I-4m2$ -BCN exhibits a large anisotropy in its Poisson ratio, shear modulus and the Young modulus.

#### 4. Summary

In summary, a theoretical study on the thermodynamic properties of  $I-4m2$ -BCN at high pressure and temperature has been undertaken using the quasi-harmonic Debye model. The structural properties in the  $I-4m2$  phase are obtained using the total energy as a function of volume and  $V/V_0$ . The calculated elastic constants are satisfying the mechanical stability conditions. It is also found that the pressure and temperature have important effects on the heat capacity, entropy, and the Gibbs free energy. Other thermodynamic properties including the Debye temperature, the Grüneisen parameter, and the

thermal expansion coefficients of  $I-4m2$ -BCN are predicted under high temperature and high pressure. High pressure leads to a smaller Grüneisen parameter, heat capacity, and thermal expansion coefficients at a given temperature. On the contrary, high temperature leads to a larger Grüneisen parameter, a larger heat capacity, and a larger thermal expansion coefficient at certain pressure. However, there are no experimental data available related to the thermodynamic properties of  $I-4m2$ -BCN at high pressure and high temperature. Moreover,  $I-4m2$ -BCN exhibits a large anisotropy in its Poisson's ratio, shear modulus and Young's modulus. Hence, we hope that our work can give more insight into the thermodynamic properties of  $I-4m2$ -BCN and will stimulate further experimental study on it.

#### Acknowledgments

This work is supported by the National Nature Science Fund (No. 61006028), and the National Nature Science Fund (No. 61204044).

#### References

- [1] Y. Yap, *B-C-N Nanotubes and Related Nanostructures*, Vol. 6, Springer, Science Business Media, New York 2009.
- [2] M.O. Watanabe, S. Itoh, K. Mizushima, T. Sasaki, *Appl. Phys. Lett.* **68**, 2962 (1996).
- [3] D. Hegemann, R. Riedel, W. Dressler, C. Oehr, B. Schindler, H. Brunner, *Chem. Vap. Depos.* **3**, 257 (1997).
- [4] C. Morant, P. Prieto, J. Bareno, J.M. Sanz, E. Elizalde, *Thin Solid Films* **515**, 207 (2006).
- [5] J. Yu, E.G. Wang, *Appl. Phys. Lett.* **74**, 2948 (1999).
- [6] J. Yu, E.G. Wang, J. Ahn, S.F. Yoon, Q. Zhang, J. Cui, M.B. Yu, *J. Appl. Phys.* **87**, 4022 (2000).
- [7] M. Kawaguchi, *Adv. Mater.* **9**, 615 (1997).
- [8] T. Sugino, Y. Etou, T. Tai, H. Mori, *Appl. Phys. Lett.* **80**, 649 (2002).
- [9] D.H. Kim, E. Byon, S. Lee, J.K. Kim, H. Ruh, *Thin Solid Films* **447**, 192 (2004).
- [10] Z.J. Zhang, C. Kimura, T. Sugino, *J. Appl. Phys.* **98**, 036105 (2005).
- [11] L. Qin, J. Yu, S.Y. Kuang, C. Xiao, X.D. Bai, *Nanoscale* **4**, 120 (2012).
- [12] M.N. Oliveira, O. Conde, *J. Mater. Res.* **16**, 734 (2001).
- [13] Z.X. Cao, H. Oechsner, *J. Appl. Phys.* **93**, 1186 (2003).
- [14] Y. Zhang, H. Sun, Ch.F. Chen, *Phys. Rev. Lett.* **93**, 195504 (2004).
- [15] F. Zhou, K. Adachi, K. Kato, *Thin Solid Films* **497**, 210 (2006).
- [16] E. Byon, J. Kim, S. Lee, J. Hah, K. Sugimoto, *Surf. Coat. Technol.* **169/170**, 340 (2003).
- [17] Q.Y. Fan, Q. Wei, C.C. Chai, X.H. Yu, Y. Liu, P.K. Zhou, H.Y. Yan, D.Y. Zhang, *Chin. J. Phys.* **53**, 100601 (2015).

- [18] Q.Y. Fan, Q. Wei, C.C. Chai, Y.T. Yang, X.H. Yu, Y. Liu, J.P. Zheng, P.K. Zhou, D.Y. Zhang, *Acta Phys. Pol. A* **129**, 103 (2016).
- [19] D.Y. Wang, Q. Yan, B. Wang, Y.X. Wang, J.M. Yang, G. Yang, *J. Chem. Phys.* **140**, 224704 (2014).
- [20] J. Chang, Y. Cheng, M. Fu, *J. At. Mol. Sci.* **1**, 243 (2010).
- [21] Q.Y. Fan, Q. Wei, C.C. Chai, H.Y. Yan, M.G. Zhang, Z.Z. Lin, Z.X. Zhang, J.Q. Zhang, D.Y. Zhang, *J. Phys. Chem. Solids* **79**, 89 (2015).
- [22] X. Zhang, Y. Wang, J. Lv, C. Zhu, Q. Li, M. Zhang, Q. Li, Y. Ma, *J. Chem. Phys.* **138**, 114101 (2013).
- [23] Q.Y. Fan, Q. Wei, C.C. Chai, M.G. Zhang, H.Y. Yan, Z.X. Zhang, J.Q. Zhang, D.Y. Zhang, *Comput. Mater. Sci.* **97**, 6 (2015).
- [24] W. Kohn, J. Sham, *Phys. Rev.* **140**, A1133 (1965).
- [25] P. Hohenberg, W. Kohn, *Phys. Rev.* **136**, B864 (1964).
- [26] J.P. Perdew, K. Burke, M. Ernzerhof, *Phys. Rev. Lett.* **77**, 3865 (1996).
- [27] S.J. Clark, M.D. Segall, C.J. Pickard, P.J. Hasnip, M.I.J. Probert, K. Refson, M.C. Payne, *Z. Kristallogr.* **220**, 567 (2005).
- [28] H.J. Monkhorst, J.D. Pack, *Phys. Rev. B* **13**, 5188 (1976).
- [29] B.G. Pfrommer, M. Côté, S.G. Louie, M.L. Cohen, *J. Comput. Phys.* **131**, 516233 (1997).
- [30] C.M. Liu, N.N. Ge, Zh.J. Fu, Y. Cheng, J. Zhu, *Chin. Phys. B* **20**, 045101 (2011).
- [31] F. Peng, H.Z. Fu, X.D. Yang, *Solid State Commun.* **145**, 91 (2008).
- [32] F. Peng, H.Z. Fu, X.D. Yang, *Phys. B* **403**, 2851 (2008).
- [33] Y. Cheng, L.Y. Lu, O.H. Jia, X.R. Chen, *Chin. Phys. B* **17**, 1355 (2008).
- [34] M.A. Blanco, Ph.D. Thesis, Universidad de Oviedo, 1997.
- [35] M.A. Blanco, A. Martín Pendás, E. Francisco, J.M. Recio, R. Franco, *J. Mol. Struct. Theochem.* **368**, 245 (1996).
- [36] E. Francisco, J.M. Recio, M.A. Blanco, A. Martín Pendás, *J. Phys. Chem.* **102**, 1595 (1998).
- [37] S. La Placa, B. Post, *Acta Crystallogr.* **15**, 97 (1962).
- [38] M. Flórez, J.M. Recio, E. Francisco, M.A. Blanco, A. Martín Pendás, *Phys. Rev. B* **66**, 144112 (2002).
- [39] E. Francisco, G. Sanjurjo, M.A. Blanco, *Phys. Rev. B* **63**, 094107 (2001).
- [40] M.A. Blanco, E. Francisco, V. Luaña, *Comput. Phys. Commun.* **158**, 57 (2004).
- [41] P. Ravindran, L. Fast, P.A. Korzhavyi, B. Johansson, J. Wills, O. Eriksson, *J. Appl. Phys.* **84**, 4891 (1998).
- [42] J.F. Nye, *Physical Properties of Crystals*, Oxford University Press, Oxford 1985.
- [43] F.D. Murnaghan, *Proc. Natl. Acad. Sci. USA* **30**, 244 (1944).
- [44] W. Greiner, L. Neise, H. Stöcker, *Thermodynamics and Statistical Mechanics*, Springer-Verlag, New York 1995, p. 101.
- [45] P. Perrot, *A to Z of Thermodynamics*, Oxford University Press, Oxford 1998.
- [46] A. Marmier, Z.A.D. Lethbridge, R.I. Walton, C.W. Smith, S.C. Parker, K.E. Evans, *Comput. Phys. Commun.* **181**, 2102 (2010).